



**Mechanical Constitutive Laws for the Irradiation
Behavior of Graphite**

R.D. Watson and W.G. Wolfer

January 1979

UWFDM-299

J. Nucl. Matls. 85 & 86, 159 (1979).

FUSION TECHNOLOGY INSTITUTE

UNIVERSITY OF WISCONSIN

MADISON WISCONSIN

Mechanical Constitutive Laws for the Irradiation Behavior of Graphite

R.D. Watson and W.G. Wolfer

Fusion Technology Institute
University of Wisconsin
1500 Engineering Drive
Madison, WI 53706

<http://fti.neep.wisc.edu>

January 1979

UWFDM-299

"LEGAL NOTICE"

"This work was prepared by the University of Wisconsin as an account of work sponsored by the Electric Power Research Institute, Inc. ("EPRI"). Neither EPRI, members of EPRI, the University of Wisconsin, nor any person acting on behalf of either:

"a. Makes any warranty or representation, express or implied, with respect to the accuracy, completeness, or usefulness of the information contained in this report, or that the use of any information, apparatus, method, or process disclosed in this report may not infringe privately owned rights; or

"b. Assumes any liabilities with respect to the use of, or for damages resulting from the use of, any information, apparatus, method or process disclosed in this report."

MECHANICAL CONSTITUTIVE LAWS FOR THE
IRRADIATION BEHAVIOR OF GRAPHITE

R.D. Watson
W.G. Wolfer

Nuclear Engineering Dept.
University of Wisconsin
Madison WI 53706 U.S.A.

January 1979

UWFD-299

MECHANICAL CONSTITUTIVE LAWS FOR THE IRRADIATION BEHAVIOR OF GRAPHITE

R. D. WATSON and W. G. WOLFER

Nuclear Engineering Department, University of Wisconsin, Madison, Wisconsin 53706 U.S.A.

Models are developed for the radiation-induced volume changes of graphite. The change in porosity is described as a two-stage process, each being associated with different types of pores in a polycrystalline graphite material. Changes in the effective elastic properties are then related to the changes in porosity and the changes in the shape of the pores. Finally, the fracture strength is shown to be related to the effective elastic properties and the size of the microcracks. The significance of the interrelationships between volume changes, elastic and fracture properties are discussed in view of fusion reactor applications.

1. INTRODUCTION

Graphite is receiving much attention as a structural material for fusion reactors because of its high melting point, its low radioactivity after neutron exposure, and because of its excellent thermal shock resistance. These positive attributes are however contrasted by its intrinsic radiation-induced instability, which is caused by the anisotropic growth of its crystallites. Inevitably, this instability leads eventually to a degradation of vital mechanical properties, such as strength, and hence, to a finite lifetime of any graphite structure after prolonged neutron irradiation.

When using graphite as a structural material in a fusion reactor, one must carefully weigh the advantages gained by the positive attributes against the finite lifetime of this material. To determine the latter, a structural analysis must be carried out as a function of the radiation exposure and the reactor operation cycle. Such an analysis was recently performed by the authors [1] for the first wall and blanket structure of the SOLASE laser fusion reactor. In spite of the fact that this analysis was applied to a specific design, the following general results and insights were obtained.

- a) Nuclear type graphite is a promising structural material for the first wall and the blanket of a fusion reactor.
- b) The lifetime of the first wall and the blanket structure made of graphite is expected to be between 5 and 10 MWyr/m² based on our previous analysis [1].
- c) The lifetime is not determined by a single property, but by the subtle interplay of radiation-induced dimensional changes in the temperature and neutron flux gradients, of strength degradations, and of the reversal of thermal stresses upon shut-down of the reactor.

- d) Premature failures and unacceptably short lifetimes of a graphite structure are possible if unfavorable combinations of dimensional changes and temperature and neutron flux gradients are encountered. These, of course, must be avoided through judicious design.
- e) Because of this subtle interplay, it is essential to recognize and properly describe the interrelationships of various materials properties as a function of neutron damage.

In the present paper we shall concentrate on this latter problem and present some new results on interrelating porosity changes with elastic and fracture property changes of graphites. Although these interrelationships have been known to exist, little work has been reported in the past to explain them on theoretical grounds or to provide the quantitative description for it.

As indicated in Fig. 1, the constitutive laws important to structural analysis fall into five groups. The solid lines connecting them indicate interrelationships which have a firm theoretical and/or empirical basis, whereas dashed lines indicate conjectured interrelationships for which little experimental evidence exists yet. We shall omit any further discussions on these conjectured relationships and only point out that they are expected to exist on grounds of theoretical considerations.

Also not included in our further discussions are properties such as the thermal conductivity and the thermal expansion coefficients. Furthermore, we restrict our efforts to isotropic graphites. However, the results can be generalized in principle to anisotropic graphites.

2. DIMENSIONAL CHANGES

The dimensional changes of polycrystalline graphites during neutron irradiation are characterized by an initial densification followed by an expansion at higher radiation doses.

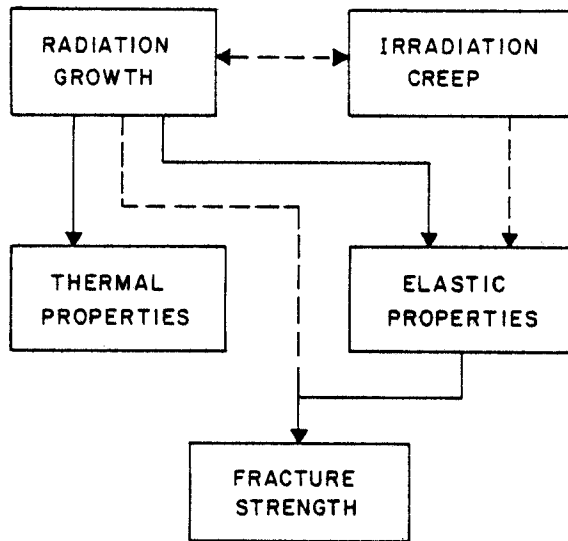


Fig. 1. Interrelationships of the properties of graphite.

This phenomenon can be explained by the dimensional changes of the graphite crystallites that make up the graphite particles and by the closure and expansion of pores and microcracks. Following the notation of Engle [2], there are three different types of pores. The crystallites themselves contain micropores which contribute the amount P_1 to the total porosity. Many crystallites are contained in a single graphite particle, and transgranular microcracks between the crystallites occupy a volume fraction P_2 . In turn, the particles are held together by a graphite binder, produced from coal-tar pitch, and they may enclose intergranular microcracks which take up the volume fraction P_3 .

During irradiation the individual crystallites expand in the c-direction, i.e., perpendicular to the basal planes, but contract parallel to the basal planes (or in the a-direction). As a result, the different pore volumes change with time. Initially, the dimensional changes are produced by a partial closure of all three pore types. However, as the crystallites continue to expand in the c-directions, new and old microcracks open up, causing P_2 and P_3 to increase.

Engle [2] found that P_1 increases slightly initially and changes little thereafter. However, P_2 decreases initially, contributing mostly to the initial densification phase, and then increased moderately at higher doses. The pore volume fraction P_3 changes little during the densification phase but then increases dramatically. Therefore, P_3 is the major contributor to the final expansion rate of graphite under irradiation.

Based on these observations one can quantify the dimensional changes by a two-step process. Initially, the densification is mainly due to a partial closure of the fabricated porosity, $(P_1 + P_2)$, which accommodates the dimensional changes of the crystallites. After exhaustion of this process, further accommodation can only be accomplished by creation of new, and enlargement of, existing microcracks, P_3 , between the particles and crystallites. It is reasonable to assume that the initial densification rate is proportional to the initial porosity, P_0 , but the final expansion rate should not depend on P_0 . However, the onset of expansion is delayed with increasing initial porosity P_0 .

A phenomenological equation, reflecting this behavior, is given by

$$P - P_0 = P_3 + (P_1 + P_2 - P_0) = \frac{AF^{n+1}}{BP_0 + F^n} - P_0 [1 - \exp(-CF)] \quad (1)$$

where F is the radiation dose, and A , B , C and n are materials parameters which must be determined by fitting Eq. (1) to the experimental data. The particular dose dependence chosen for the first term in Eq. (1) is based on the assumption that the volumetric expansion due to P_3 will eventually become linear with dose. At present, there is no data at high doses available that either contradict or confirm this conjecture. However, it appears reasonable to assume that the expansion of the crystallites along their c-axis must eventually be linear with dose.

The dimensional changes of a particular graphite depend strongly on the raw material and the fabrication process used. Therefore, the parameters in Eq. (1) were selected such that Eq. (1) fits a variety of different graphites. By inspection of available data and various forms of Eq. (1), it was determined that the equation

$$P - P_0 = \frac{\Delta V}{V_0} = \frac{AF^3}{P_0/C + F^2} - P_0 [1 - \exp(-CF)] \quad (2)$$

is the most compatible with the entire body of data utilized. Equation (2) contains only two parameters, A and C , which must be determined from experimental data. The most convenient way to accomplish this is to compare the initial shrinkage rate and the final growth rate with the data, since $\dot{P}(0) = -P_0C$ and $\dot{P}(F \rightarrow \infty) = A$. The data that were used to determine A and C were length changes of anisotropic graphites [4,5,6]. Therefore, the volume changes $\Delta V/V_0$ were computed from the length changes $(\Delta L/L)_{\parallel}$ parallel and the length changes $(\Delta L/L)_{\perp}$ perpendicular to the extrusion direction according to the formula

$$P - P_0 = \frac{\Delta V}{V_0} = \left(\frac{\Delta L}{L}\right)_{\parallel} + 2\left(\frac{\Delta L}{L}\right)_{\perp} \quad (3)$$

Conversion from fluence units to displacements per atom (dpa) was made according to correlations of Morgan [3]. The final growth rates for the length changes were estimated from the

curves reported in the literature, and the volumetric growth rates were then computed with Eq. (3). These values are plotted in Fig. 2. The same procedure was followed for obtaining the initial shrinkage rates. The corresponding values are plotted in Fig. 3.

According to Fig. 2, it appears that one can divide the different graphites into two groups. The group comprising the majority of the data in Fig. 2 has a modest final growth rate with a maximum of about 1.5 ($\Delta V/V_0$ %)/dpa at 1000°C. Both data groups were fitted to simple analytical expressions. For the low-growth graphites

$$A = \left\{ \left(\frac{800}{T} \right)^2 + \left(\frac{T}{1250} \right)^2 \right\}^{-1} \left[\frac{\Delta V}{V_0} \% / \text{dpa} \right] \quad (4)$$

where T is the temperature in °C, and for the high growth graphites

$$A = 9.4 \left\{ \left(\frac{900}{T} \right)^6 + \left(\frac{T}{1050} \right)^4 \right\}^{-1} \left[\frac{\Delta V}{V_0} \% / \text{dpa} \right]. \quad (5)$$

Contrary to the distinction in the final growth rate, the graphites considered for this study do not differ in their initial shrinkage rates, as can be clearly seen from Fig. 3. Therefore, all the data can be fitted to one expression. The nominal or average fit is simply given by

$$C = 0.01 \left(\frac{T-700}{210} \right)^2 + 0.02. \quad (6)$$

A lower bound can be obtained from

$$C = 0.01 \left(\frac{T-700}{230} \right)^2, \quad (6a)$$

and an upper bound from

$$C = 0.01 \left(\frac{T-700}{170} \right)^2 + 0.04. \quad (6b)$$

3. ELASTIC CHANGES

There exists an extensive literature on the effective elastic moduli of heterogeneous materials in terms of the moduli of the crystalline phases and their volume fractions. Pores are treated in this context as a phase with vanishing elastic constants. In a different approach one computes the effective moduli from the strain energy of a solid with N cracks per unit volume. It appears to us that the latter approach is more appropriate for graphite. Accordingly, we adopt the recent theoretical results derived by Budianski and O'Connell [7]. As they have shown, elliptical cracks give results very similar to circular ones. Accordingly, we assume that the porosities ($P_1 + P_2$) can be modelled as N_1 cracks with radius a_1 and height c_1 , and P_3 as N_3 cracks with radius a_3 and height c_3 . The crack-density parameter

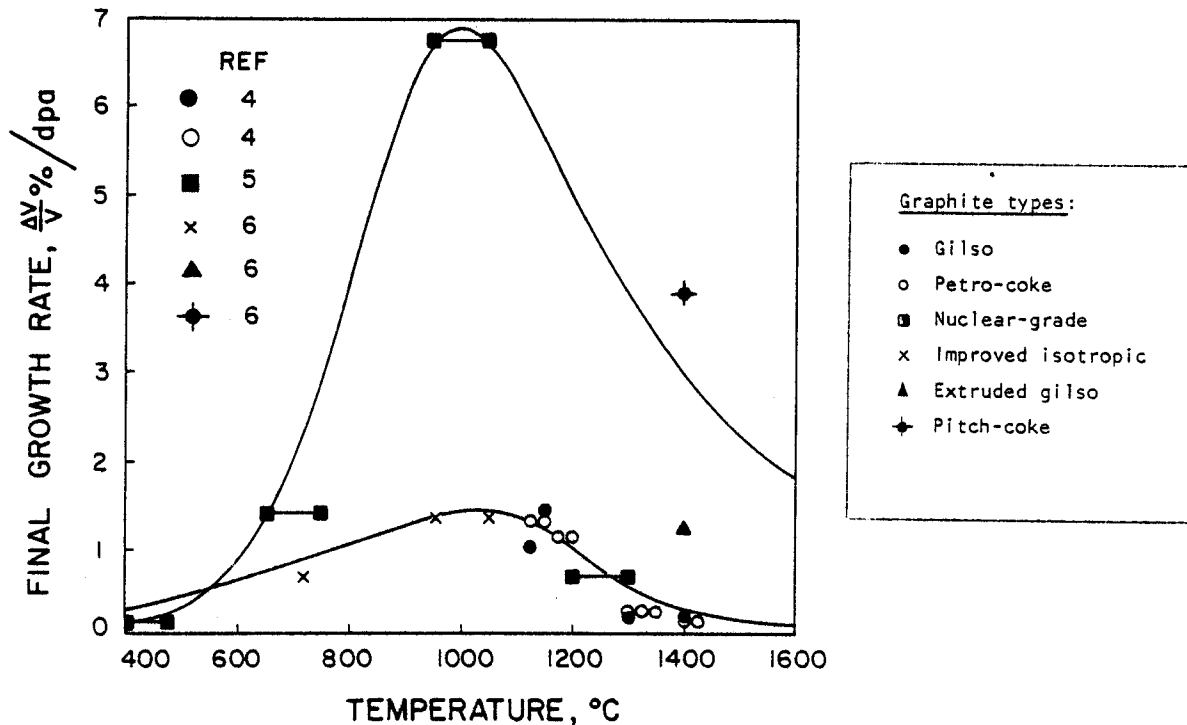


Fig. 2. Final volumetric growth rate of various graphites as a function of irradiation temperature.

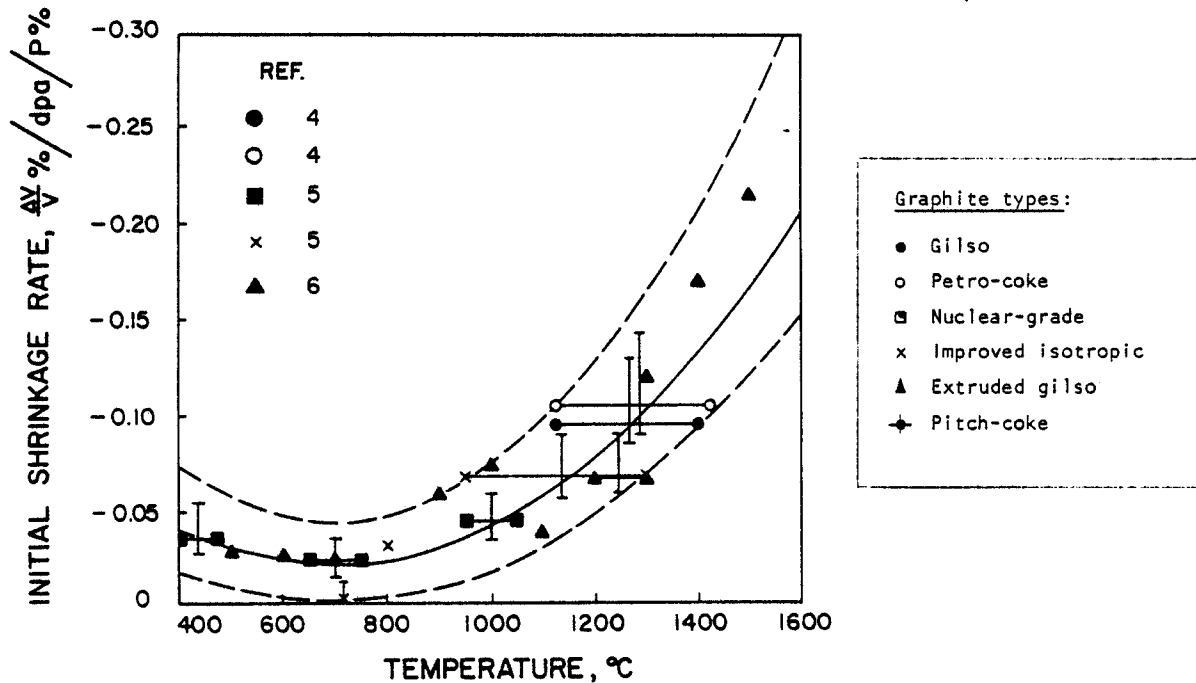


Fig. 3. Initial volumetric shrinkage rates of various graphites as a function of irradiation temperature.

$$\eta = N\bar{a}^3 = N_1 a_1^3 + N_3 a_3^3, \quad (7)$$

where N is the total number of cracks per unit volume, can then be expressed in terms of the porosities as

$$\begin{aligned} \eta &= N_1 \pi a_1^2 c_1 f_1 + N_3 \pi a_3^2 c_3 f_3 = (P_1 + P_2) f_1 + P_3 f_3 \\ &= N \pi \bar{a}^2 \bar{c} \bar{f} = P \bar{F}, \end{aligned} \quad (8)$$

where $f_1 = a_1/\pi c_1$, $f_3 = a_3/\pi c_3$, $\bar{f} = \bar{a}/\pi \bar{c}$ are pore shape parameters, and $P = P_1 + P_2 + P_3$ is the total porosity. The average shape parameter can be written as

$$\bar{F} = [f_1 P_0 \exp(-CF) + f_3 P_3] / [P_0 \exp(-CF) + P_3] \quad (9)$$

when using Eq. (2).

The effective elastic moduli for the cracked solid are given as functions of the crack-density parameter η and the elastic constants for a theoretically dense isotropic graphite. If we denote the latter ones by E, ν , then the effective Poisson's ratio $\bar{\nu}$ is the solution of the equation [7]

$$\frac{16}{45} \eta (1 - \bar{\nu}^2) [10\bar{\nu} - \bar{\nu}(1+3\nu)] = (\nu - \bar{\nu})(2 - \bar{\nu}) \quad (10)$$

and the effective Young's modulus \bar{E} is given by [7]

$$\bar{E}/E = 1 - \frac{16}{45} \eta (1 - \bar{\nu}^2) (10 - 3\bar{\nu}) / (2 - \bar{\nu}) \quad (11)$$

Within an accuracy of 3%, the much simpler equation

$$\bar{E}/E \approx 1 - \frac{16}{9} P \bar{F} \quad (12)$$

approximates Eq. (11). Similarly,

$$\bar{\nu} \approx \nu (1 - \frac{16}{9} P \bar{F}) \quad (13)$$

underpredicts the exact solution by at most 4% provided $\nu \leq 0.4$. In the last two equations $P \bar{F}$ was substituted for η from Eq. (8), and P is given by Eq. (2).

To complete the description, specific values must be determined for the shape parameters f_1 and f_3 . This was accomplished by comparing the volume changes with the changes of the Young's modulus measured on the same irradiated samples

of graphite [8]. From Eq. (12) one obtains

$$\bar{f} = \frac{9}{16} (1 - \bar{E}/\bar{E}_0) / (P - P_0 \bar{E}/\bar{E}_0) \quad (14)$$

where \bar{E}_0 is the Young's modulus for the graphite with the original porosity P_0 .

Because of the effect of dislocation pinning, the elastic modulus changes at first rapidly and levels off after an irradiation dose of about 2 dpa [9]. Any subsequent changes in \bar{E} are due to porosity changes. Hence \bar{E}_0 is the value of the Young's modulus after dislocation pinning has occurred. Using the data of Ref. 8, the average pore shape parameter \bar{f} was computed according to Eq. (14), and plotted in Fig. 4. Due to the large scatter in the data for both P and \bar{E} , there is a correspondingly large uncertainty in \bar{f} . Nevertheless, the data clearly indicate that \bar{f} changes from an initial value f_1 to a final value f_3 in accordance with Eq. (9). In fact, by using an equation of the form of Eq. (2) to describe the measured porosity P for the data of Ref. 8, \bar{f} was computed from Eq. (9). The curves in Fig. 4 show the computed values of \bar{f} for $f_1 = 1.5$ and $f_3 = 3$. The result, namely that the pore shape of the original porosity is closer to being spherical than the cracks developed later on, is in agreement with the microstructural observations of Engle [2].

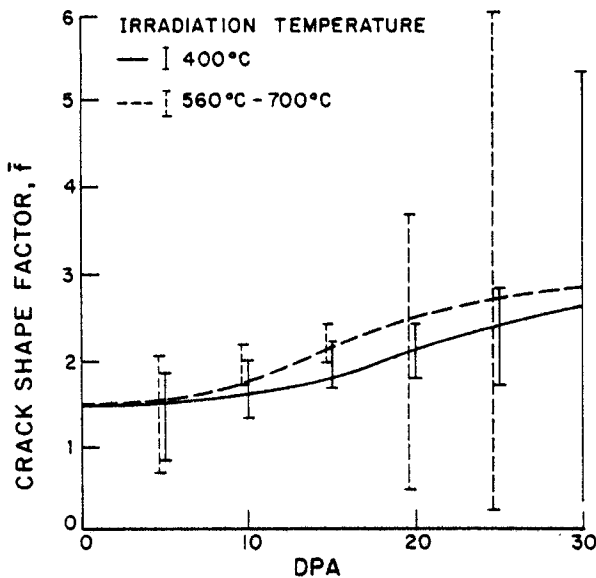


Fig. 4. Change of the average crack shape factor \bar{f} as a function of the neutron irradiation dose.

4. FRACTURE STRENGTH

It is quite obvious from the theoretical approach by Budianski and O'Connell [7], for the elastic moduli of a crack solid, that a close relationship must exist between the elastic properties and the static fracture properties. In fact, using their expression for the stored elastic energy and the Griffith fracture criterion, we find that the fracture strength is given by

$$\sigma^f = \left[\frac{\pi \gamma \bar{E}}{2a(1-\nu^2)} \right]^{1/2}$$

where γ is the surface energy.

Relative to the original fracture strength σ_0^f , σ^f can be obtained from

$$\sigma^f / \sigma_0^f = \left[\frac{\bar{E}(1-\nu_0^2)a_0}{\bar{E}_0(1-\nu^2)a} \right]^{1/2} \approx \left[\frac{\bar{E}a_0}{\bar{E}_0 a} \right]^{1/2} \quad (15)$$

The last expression is a good approximation since $\nu_0^2 \approx \nu^2 \ll 1$.

As long as the crack radius does not change in the course of the dimensional changes, $a = a_0$, and $\sigma^f \sim \sqrt{\bar{E}}$. This behavior has indeed been observed [9] over irradiation doses where shrinkage and modest growth occurs. However, at very high doses where large pores develop and where the crack size a increases, σ^f decreases more rapidly, and the observations suggest a relationship of the form $\sigma^f \sim \bar{E}$. The latter, however, must be considered empirical in view of Eq. (15).

5. DISCUSSION

In order to relate the radiation-induced dimensional changes with the elastic and fracture properties, it is necessary to characterize the microstructure of graphite in terms of the volume fractions of the original and the radiation-induced porosity, together with the corresponding pore shape factors. In the case of the fracture strength, however, the major pore radius "a" would also be required as an additional parameter in order to predict the fracture strength for large neutron fluences.

The need for more microstructural information on irradiated graphite is even greater if one desires to model anisotropic graphites. In this case the probability distribution for the grain orientation and the microcrack orientation must be known in order to compute the anisotropic elastic constants and the fracture strength tensor. Such information can be obtained on very small samples, and the successful prediction of mechanical properties from it may obviate testing on large irradiated specimens.

In addition to the improvements needed to model anisotropic graphites, the program of relating microstructure to properties must also

be extended to include irradiation creep, the effect of stress on dimensional changes, thermal expansion, and thermal conductivity. As stated in the introduction, a self-consistent description of these properties and their interrelations is essential to the structural and lifetime analysis of graphite-components in fusion reactors.

ACKNOWLEDGEMENT

This work was supported by the Electric Power Research Institute under contract # RP-237-3.

REFERENCES

1. W.G. Wolfer and R.D. Watson, Proc. 3rd Topical Meeting on the Technology of Controlled Nuclear Fusion, Santa Fe, 1978, CONF-780508, Vol. 1, p. 289.
2. G.B. Engle, Carbon 9, (1971), 539.
3. W.C. Morgan, Nucl. Technology 21, (1974), 50.
4. W.C. Morgan, E.M. Woodruff, and W.J. Gray, Techn. of Controlled Nuclear Fusion, Vol. 1, CONF-760935-P1 (1976), 189.
5. W.J. Gray and W.C. Morgan, Techn. of Controlled Thermonuclear Fusion Experiments and Engineering Aspects of Fusion Reactors, CONF-721111 (1972), 983.
6. M. Van den Berg, M.R. Everett, and A. Kingery, Proc. of the 12th Biennial Conf. on Carbon, Pittsburgh (1975), 307.
7. B. Budianski and R.J. O'Connell, Int. J. Solids Structures 12, (1976), 91.
8. P.T. Nettle, J.E. Brocklehurst, W.H. Martin, and J.H.W. Simmons, IAEA Symp. Advanced High Temp. Gas Cooled Reactors, IAEA Vienna (1969), 604.
9. J.E. Brocklehurst, Chemistry and Physics of Carbon 13, (1977), 145.